Fall 2013

The Deletion of the Bre1 Gene in Aspergillus nidulans Impairs Mitotic Growth, Meiosis, and DNA Damage Repair

Andrea J. Sitton
Gettysburg College

Steven W. James
Gettysburg College

The Deletion of the Bre1 Gene in Aspergillus nidulans Impairs Mitotic Growth, Meiosis, and DNA Damage Repair

Abstract
Bre1 is a homotetrameric E3 ubiquitin-protein ligase that heterodimerizes with Rad6, an E2 ubiquitin-conjugating enzyme, in order to ubiquitinate lysine 123 in Aspergillus nidulans. This post-translational modification promotes methylation of lysines 4 and 79 on histone H3, which are required for certain damage repair pathways and for both optimal mitotic cell growth and meiosis [1-3, 12]. ΔBre1 mutants were generated by exposing protoplasts from strains auxotrophic for pyridoxine to a three-way fusion construct made from the Bre1 5' and 3' flanking regions and the Aspergillus fumigatus pyroA gene, which served as a selectable marker. Molecular diagnosis was confirmed via trans-locus PCR. Phenotypic analysis indicates that the loss of Bre1 increases sensitivity to DNA damage agents, decreases mitotic cell growth, and inhibits meiosis. The severe developmental defects of ΔBre1 mutants are consistent with the known roles of Bre1 as an upstream regulator of several important cellular functions. [*excerpt*]

Keywords
gene deletion; Bre1; Aspergillus nidulans; RNF20; RNF40, Stock Writing Prize

Disciplines
Biology

Comments
Winner of the 2014 Stock Writing Prize for Sciences

The deletion of the Bre1 gene in *Aspergillus nidulans* impairs mitotic growth, meiosis, and DNA damage repair

Andrea Sitton

Dr. Steven W. James

Department of Biology
Gettysburg College
Gettysburg, PA 17325

Abstract

Bre1 is a homotetrameric E3 ubiquitin-protein ligase that heterodimerizes with Rad6, an E2 ubiquitin-conjugating enzyme, in order to ubiquitinate lysine 123 in *Aspergillus nidulans.* This post-translational modification promotes methylation of lysines 4 and 79 on histone H3, which are required for certain damage repair pathways and for both optimal mitotic cell growth and meiosis [1-3, 12]. ΔBre1 mutants were generated by exposing protoplasts from strains auxotrophic for pyridoxine to a three-way fusion construct made from the Bre1 5' and 3' flanking regions and the *Aspergillus fumigatus pyroA* gene, which served as a selectable marker. Molecular diagnosis was confirmed via trans-locus PCR. Phenotypic analysis indicates that the loss of Bre1 increases sensitivity to DNA damage agents, decreases mitotic cell growth, and inhibits meiosis. The severe developmental defects of ΔBre1 mutants are consistent with the known roles of Bre1 as an upstream regulator of several important cellular functions.

Introduction

Bre1 is a homotetrameric E3 ubiquitin-protein ligase, containing four identical Bre1 peptides in *Saccharomyces cerevisiae* and two each of Rnf20 and Rnf40 peptides in the *Homo sapiens* ortholog, that heterodimerizes with Rad6, an E2 ubiquitin-conjugating enzyme, in order to ubiquitinate lysine 123 (in *S. cerevisiae*) or lysine 120 (in *H. sapiens*) on histone H2B, which then promotes methylation of lysines 4 and 79 on histone H3; these post-translational modifications are found in areas of active transcription, and are required for certain damage repair pathways [1-3]. The Spt-Ada-Gcn5-acetyltransferase (SAGA) complex associates with Ubp8 to deubiquitinate histone H2B-K123, reversing the actions of Bre1; its deubiquitination activity is regulated by Lge1 [4].

Rad6 associates with Bre1 through the N-terminal region of Bre1, and the Bre1-Rad6 complex then associates with the Lge1 protein, which is a protein of unknown function but is necessary for the Bre1 ubiquitination ligase activity [2, 4]. Bre1 directs the Bre1-Rad6-Lge1 complex to the promoter region

of a gene about to be transcribed, and the complex associates with the transcription preinitiation complex. This association sets off a chain reaction through which Paf1, COMPASS (especially the Swd2 subunit), and Dot1 complexes are recruited and facilitate the processive elongation activity of RNA polymerase II [2, 5].

The Rtf1 and Paf1 subunits of the Paf1 complex mediate the interactions between the Bre1-Rad6-Lge1 complex, COMPASS, and RNA polymerase II, which is required for the functional activation of the Bre1-Rad6-Lge1 complex in the ubiquitination of histone H2B-K123 [2, 5]. Bre1/Rnf20 also interacts with Cdc73, a subunit of Paf1 required for significant monoubiquitination of histone H2B-K120, but not for trimethylation on histone H3-K4, indicating that monoubiquitination of histone H2B-K120 is not always necessary for trimethylation of histone H3-K4 [6]. Although the mechanism of the association of the Paf1 and Bre1-Rad6-Lge1 complexes is not well-understood, Bre1, not Rad6, is responsible for facilitating the interaction with Paf1 [2].

Monoubiquitination of histone H2B-K123 recruits the Swd2 subunit to associate with the COMPASS complex, which is necessary for the catalytic activity of COMPASS [7, 8]. The Rad6-Bre1-Lge1 complex monoubiquitinates lysines 68 and 69 of Swd2, which activates the COMPASS complex such that the dimethylation or trimethylation of histone H3-K4 can occur [7, 9]. Histone H2B-K123 ubiquitination also recruits the Dot1 complex to bind to the tail of histone H4 [10]. Independent of COMPASS activity, Dot1 methylates histone H3-K79 in a nonprocessive manner. It can be recruited again, which allows for the dimethylation or trimethylation of histone H3-K79 [10]. These post-translational modifications are necessary for the RNA pol II-COMPASS-Paf1 complex to enter processive elongation and for signaling certain DNA damage repair pathways (Figure 1) [3, 5, 11].

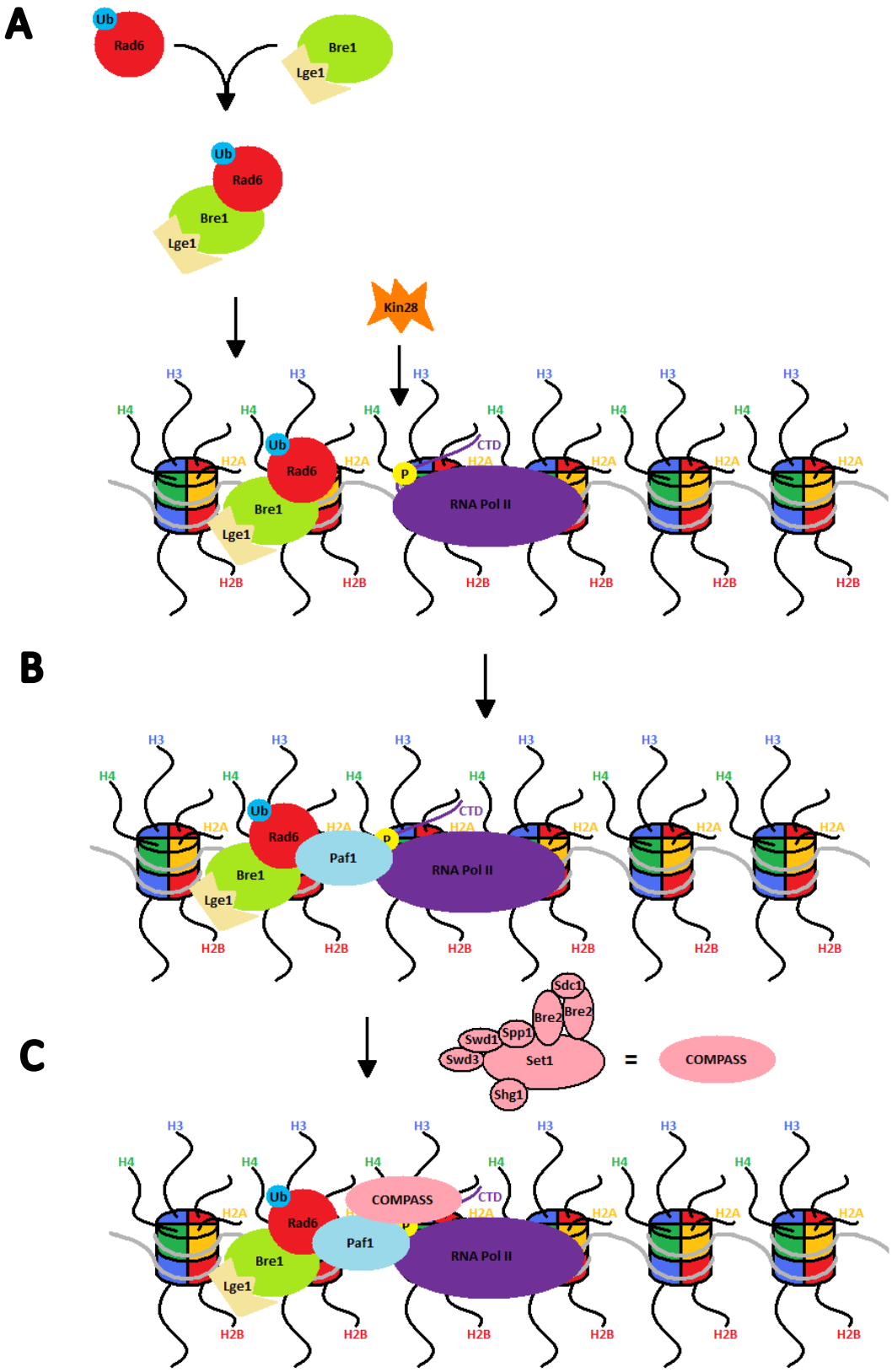
A
Ub
Rad6
Bre1
Lge1
Kin28
H3
H4
H2A
H2B
CTD
P
RNA Pol II
B
Paf1
C
Sdc1
Bre2
Swd1
Spp1
Swd3
Set1
Shg1
=
COMPASS

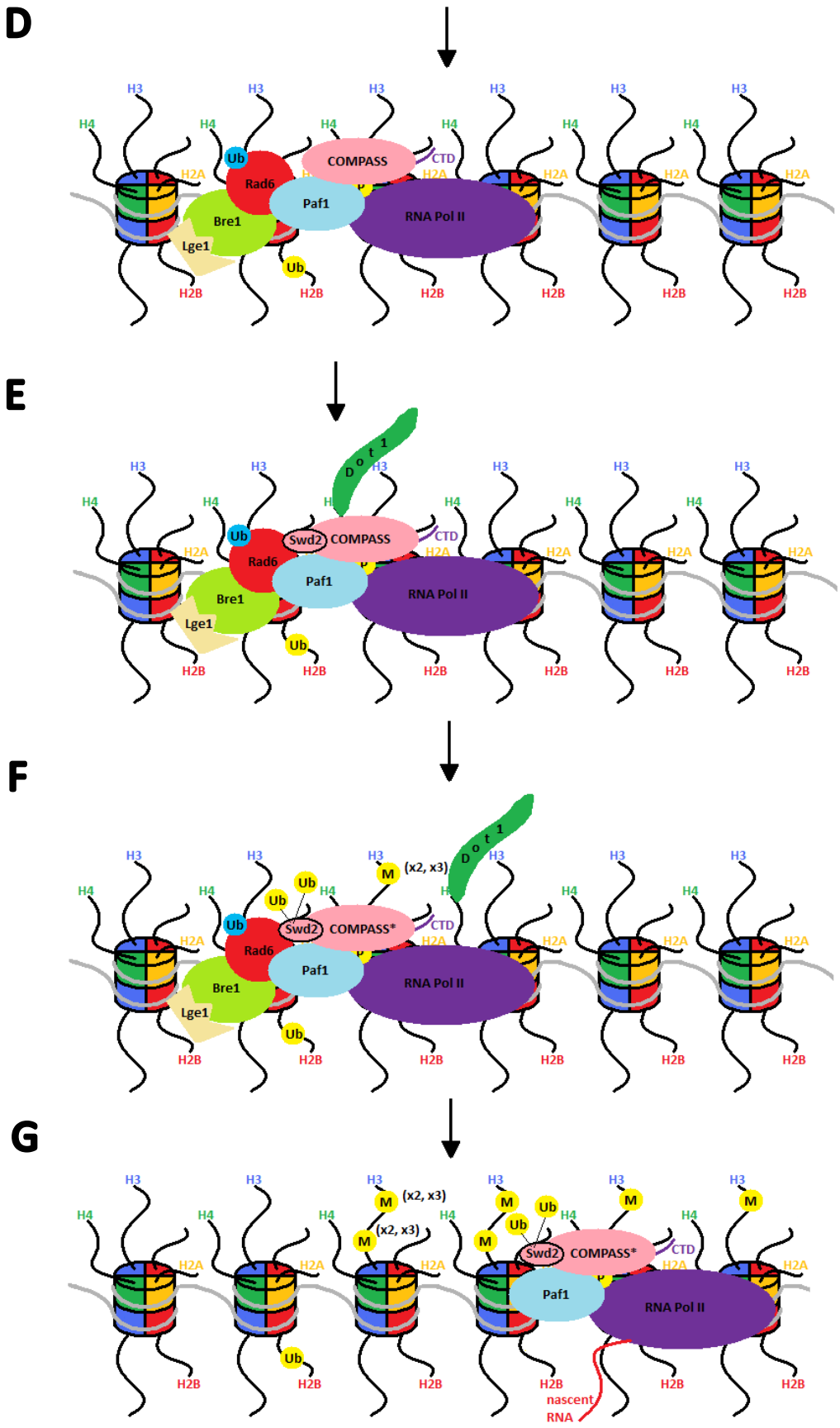
D
E
F
G
H3
H4
H2A
H2B
Ub
Rad6
Bre1
Lge1
Paf1
COMPASS
Swd2
COMPASS*
CTD
RNA Pol II
Dot1
M
(x2, x3)
nascent
RNA

Figure 1. Pathway diagram of Bre1 and its role in the ubiquitination of histone H2B and Swd2 at promoters.

A. Rad6, an E2 ubiquitin-conjugating enzyme, associates with Bre1, an E3 ubiquitin-protein isopeptide ligase. Bre1, which is associated with the Lge1 protein, binds to Rad6 via the C3HC4 RING finger domain to form the Rad6-Bre1 complex, and directs Rad6 to the promoter region of a gene about to be transcribed. Kin28 phosphorylates S5 of the CTD of RNA polymerase II after the preinitiation complex forms [1, 5, 8, 12, 13].

B. Paf1 joins the preinitiation complex and is responsible for facilitating the interactions between the Rad6-Bre1 complex and the RNA polymerase II [5].

C. Paf1 recruits members of the Set1-containing COMPASS complex, which bind to Paf1 and RNA pol II [5].

D. The assembled preinitiation complex allows the Rad6-Bre1-Lge1 complex to mono-ubiquitinate lysine 123 on histone H2B [7, 8].

E. Ubiquitination of H2BK123 recruits the Swd2 subunit to associate with the COMPASS complex, which is necessary for the catalytic activity of COMPASS. H2BK123 ubiquitination also recruits Dot1 to bind to the tail of histone H4 [7, 8, 10].

F. The Rad6-Bre1-Lge1 complex mono-ubiquitinates lysines 68 and 69 of Swd2, which activates the COMPASS complex such that the di-methylation or tri-methylation of H3K4 residues can occur. Independent of COMPASS activity, Dot1 methylates H3K79 in a nonprocessive manner, meaning it dissociates after each methylation. It can be recruited again, which allows for the di-methylation (x2) or tri-methylation (x3) of H3K79 [3, 7, 9, 11].

G. The Rad6-Bre1-Lge1 complex dissociates, and the RNA pol II-COMPASS-Paf1 complex enters elongation as COMPASS continues to methylate H3K4 residues [5].

The *Aspergillus nidulans* Bre1 protein was named for the ortholog in *Saccharomyces cerevisiae*. The orthologs in *Schizosaccharomyces pombe* and *Neurospora crassa* are called Brl2 and NCU07544, respectively. Rnf20 is the ortholog in both *Homo sapiens* and *Mus musculus*. All Bre1 orthologs contain the same conserved C3HC4 zinc finger (RING finger) domain at the C-terminal end. This RING finger is required for the monoubiquitination of histone H2B-K123 (in *S. cerevisiae*) or histone H2B-K120 (in *H. sapiens*) via the Bre1-Rad6-Lge1 complex, and this monoubiquitination is necessary for the subsequent methylations of histone H3-K4 and histone H3-K79 by other protein complexes [1, 7]. H2B ubiquitination was lost by point mutations or deletions within the RING finger, indicating that the RING finger domain is vital to the ubiquitin ligase activity of Bre1 [2]. Deletion of Bre1 in *S. cerevisiae* confers hypersensitivity to brefeldin A, cycloheximide, and chlorpromazine and sensitivity to p-chloromercuribenzoic acid, canthardate, and diphenyleneiodonium [14, 15].

The Bre1 ortholog in *H. sapiens*, Rnf20, functions as a transcriptional coactivator through direct association with p53, a well-known tumor suppressor, and is recruited to certain promoters in a p53-dependent manner [16]. Additionally, the Bre1-Rad6-Lge1 complex genetically interacts with Cdc28, the CDK that is both necessary and sufficient for cell cycle regulation in *S. cerevisiae*, by promoting expression of early cyclins [13]. Bre1 is also involved in checkpoint control, primarily through its ability to regulate dimethylation and trimethylation of histone H3-K79; deletion of Bre1 produced strains with defects in the G1 and intra-S checkpoints [11]. This deletion also imparts an increased sensitivity to X-rays due to the decrease in histone H3-K79 methylation, which is important for recruiting 53BP1 to areas containing double strand breaks [3].

In *Saccharomyces cerevisiae*, 42 physical interactions and 634 genetic interactions with Bre1 have been characterized [17]. Six physical interactions and one genetic interaction have been identified with the *Schizosaccharomyces pombe* ortholog Brl2 [18]. For *Homo sapiens* and *Mus musculus,* only physical interactions with the Rnf20 ortholog have been determined, though 66 have been discovered in humans whereas only one has been verified in mice [19, 20]. No interactions, physical or genetic, have been identified in the *Neurospora crassa* ortholog NCU07544 [21].

The interactions with the *H. sapiens* ortholog, Rnf20, can be grouped into a few distinct functional categories: histone proteins, proteins involved with ubiquitin, proteins involved in repair pathways or tumor prevention, regulatory proteins, and uncategorized “orphan” proteins. The histone proteins include HIST2H2BE, HIST1H2BN, HIST1H2BC, HIST1H2BO, HIST1H2BA, HIST1H2BK, HIST1H2BE, HIST1H2BL, HIST1H2BM, HIST2H2BF, HIST1H2BI, HIST1H2BD, HIST1H1BH, HIST2H2AA3, HIST2H2AC, HIST2H3C, HIST2H4A, HIST3H2BB, HIST1H2BG, HIST1H2BJ, and HIST1H2BB [19]. The proteins involved with ubiquitin include UBC (ubiquitin C); UBE2A, UBE2B, and UBE2E1 (E2 ubiquitin-conjugating enzymes); RNF20, RNF40, and SMURF2 (E3 ubiquitin-protein ligases); and SUMO1, SUMO2, and SUMO3 (small ubiquitin-related modifiers) [19]. The proteins involved with repair pathways or tumor prevention

include ATM (serine/threonine protein kinase activated by double strand breaks); PMS1 (thought to be involved in DNA mismatch repair); and TP53 and CDKN2B (tumor suppressors) [19]. Regulatory proteins include WAC (involved in protein-protein interactions); YWHAQ (involved in signal transduction); PAF1 (involved in regulation of transcription elongation and chromatin remodeling) and CDC73 (part of PAF protein complex); PA2G4 (involved in growth regulation); and ITSN2 (involved in regulation of formation of clathrin-coated vesicles) [19]. Other "orphan" proteins include KIF5B, MYO1E, HTT, AR, C20ORF94, and ASAP1 [19].

In this experiment, the Bre1 gene was deleted from strains of *Aspergillus nidulans* and the effect on mitotic growth, temperature sensitivity, DNA damage response, and meiotic viability was investigated.

Materials and Methods

Preparation of *Aspergillus fumigatus* DNA

To prepare the *Af pyroA* gene for use as a selectable marker in the Bre1 deletion construct, 1.65 kb region containing the *pyroA* gene was amplified via PCR and separated electrophoretically. Gel DNA purification was done by QIAEX extraction (QIAEX II Gel Extraction Kit, QIAGEN Sciences, Valencia, CA) according to the manufacturer's directions with the exception that four volumes of extraction buffer were used instead of three. Purified DNA was stained with bisbenzimide, and concentration was detected by a DyNAQuant 200 spectrophotometer (Hoefer Scientific, Holliston, MA) operated according to the manufacturer's instructions. DNA recovery was qualitatively assessed by gel electrophoresis.

PCR amplification of *Aspergillus nidulans* Bre1 5' and 3' flanks

To amplify the regions flanking the Bre1 gene for use in the Bre1 deletion construct, primers were designed using NetPrimer (Biosoft) and synthesized by Midland Certified Reagent Company (Midland, TX) (Table 1).

Table 1. PCR primers and cycling conditions.

Information regarding the *Aspergillus fumigatus pyroA* selectable marker tails is highlighted in blue. Dashes represent unavailable information.

Name	Sequence	T_m (°C)	T_A (°C)	Cycling Conditions
Af pyroA – For	5'–TAC CAC AAA TAC AAT GGC GAG AGA G–3'	63.0	-	98°C, 30 sec 98°C, 10 sec -°C, 10 sec 72°C, - } 35 cycles 72°C, -
Af pyroA – Rev	5'–GCA CAG AAC ACC CTA ACA AGA ATG AAC C–3'	68.0	-	
Bre1 – 5' For	5'–CAA AGC GTT ATT GCC TGC C–3'	59.3	60.0 (62.0)	<u>Flank Forming PCRs</u> 98°C, 30 sec 98°C, 10 sec 60°C, 10 sec 72°C, 1 min } 35 cycles 72°C, 4 min
Bre1 – 5' Rev + 3' pyroA MT	5'–GGT TCA TTC TTG TTA GGG TGT TCT GTG CTA TGG AGT GGT GAA GTC GTG AC–3'	62.7 57.3	63.0 60.0	
Bre1 – 3' For + 5' pyroA MT	5'–CTC TCT CGC CAT TGT ATT TGT GGT ACA GAG AAT GCG TGG AAG AGC–3'	67.6 58.2	63.0 60.0	<u>Three-way Fusion PCR</u> 98°C, 30 sec 98°C, 10 sec 63°C, 10 sec 72°C, 2:30 } 10 cycles 98°C, 10 sec 72°C, 3:10 } 20 cycles 72°C, 10 min
Bre1 – 3' Rev	5'–CGT GGT ACT TGT TGC TTG TGG–3'	59.0	60.0 (62.0)	
Bre1 – Ne 5' For	5'–CGT CGC TCT TCG TTG TTG A–3'	57.7	60.0	<u>Nested PCR</u> 98°C, 30 sec 98°C, 10 sec 60°C, 10 sec 72°C, 1 min } 35 cycles 72°C, 15 min
Bre1 – Ne 3' Rev	5'–AAC TGA TGA CGG TAT CTT CGG–3'	56.8	60.0	

Reaction mixtures (50 µL) included the following substituents at approximate final concentrations: BSA (0.1 mg/mL), forward and reverse primers (0.5 µM), dNTPs (0.2-0.4 mM), Phusion High Fidelity PCR reaction buffer (20 mM Tris-HCl, pH = 8.3; 3.5 mM $MgCl_2$, 100 mM KCl) (New England

BioLabs, Ipswitch, MA), Phusion Polymerase (0.5 µL) (New England BioLabs, Ipswitch, MA), template DNA (1.5 µL; 1:10 dilution), and dH_2O was used to bring the reactions to volume.

The 5' flanks of the template gDNA (PCS 439 and SWJ 400) were amplified with Bre1 – 5' For and Bre1 – 5' Rev + 3' pyroA MT, and the 3' flanks were amplified with Bre1 – 3' For + 5' pyroA MT and Bre1 – 3' Rev. Cycling conditions are listed in Table 1 and were carried out by a Bio-Rad MyCycler Thermal Cycler. The DNA was amplified, separated electrophoretically, and purified by QIAEX extraction. The two reactions were pooled, the concentration was determined, and DNA recovery was qualitatively assessed by gel electrophoresis.

Generation of the three-way fusion product

To create the three-way fusion Bre1 deletion construct, the 5' and 3' flanks were combined with the *pyroA* selectable marker in a 1:1:3 ratio (0.08 pmoles:0.08 pmoles:0.23 pmoles per 50 µL reaction) in place of primers. Otherwise, the reaction mixture was made as previously described. Cycling conditions, listed in Table 1, were modified to accommodate the length of the transcripts. The shorter cycles in the beginning facilitate formation of the two-way products, and the subsequent longer cycles generate the three-way fusion product. Presence of the three-way product was verified by gel electrophoresis. The strategy for forming the three-way product is illustrated in Figure 2.

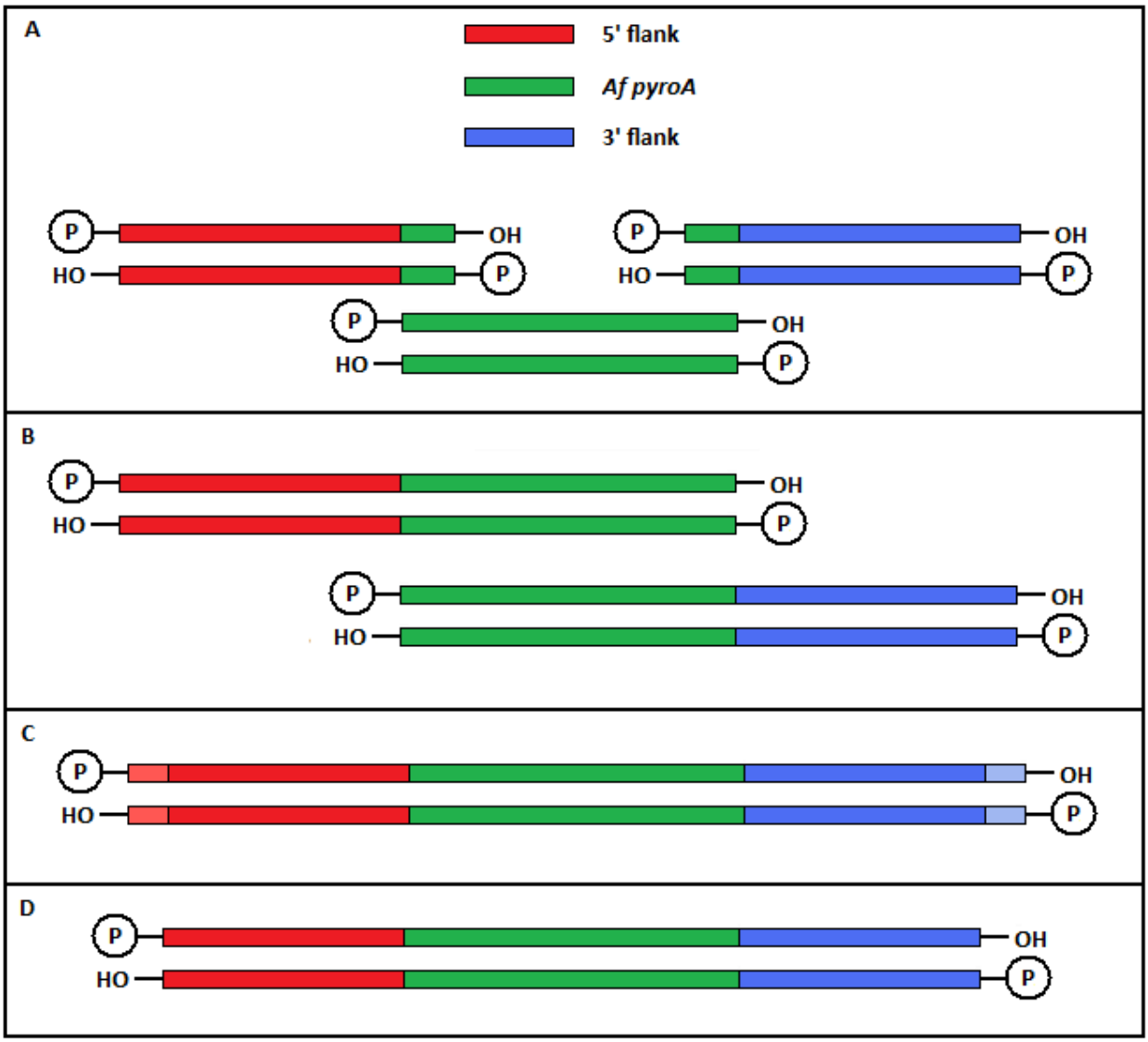

Figure 2. Strategy for the three-way fusion PCR construct.

A. The three individual amplicons: Bre1 5' flank (red), Bre1 3' flank (blue), and *Af pyroA* selectable marker (green).

B. The 2 two-way reaction products: Bre1 5' flank + *Af pyroA* and Bre1 3' flank + *Af pyroA.*

C. The initial three-way fusion product.

D. The final nested three-way fusion product.

Amplification and purification of the three-way fusion product

To prepare the deletion construct for transformation, the three-way fusion product was amplified with a set of nested primers. The reaction mixture used 2 µL of the initial three-way fusion reaction mixture as a template. Otherwise, the reaction mixture was made as previously described.

Cycling conditions are listed in Table 1. The two reactions were pooled, the concentration was determined, and DNA recovery was qualitatively assessed by gel electrophoresis. The remaining nested PCR reaction mixture was combined with 50 µL of TE and purified via phenol chloroform extraction. To the 150 µL of reaction mixture, 110 µL of phenol:chloroform:isoamyl alcohol (25:24:1) were added, and the tube was vortexed vigorously to ensure thorough mixing. The tube was centrifuged (max speed, 5 min.), and the aqueous phase was recovered and treated with 20 µL of 3M NaOAc (pH = 5.2) followed by 375 µL of 95% EtOH (-20°C). The reaction mixture was incubated at -20°C overnight to allow DNA to precipitate. Precipitated DNA was pelleted, washed twice with 70% EtOH (600 µL, -20°C), and dried in a Speed-Vac dryer at medium heat for 25 minutes. The pellet of DNA was resuspended in 10 µL of TE and 90 µL sterile dH_2O. The concentration was determined, and DNA recovery was qualitatively assessed by gel electrophoresis.

DNA-mediated transformation of *Aspergillus nidulans*

Four strains of *Aspergillus nidulans*, all auxotrophic for pyridoxine, were transformed according to the James' laboratory *Aspergillus nidulans* transformation protocol (Table 2) (S. James, pers. comm.).

Table 2. Strains used during the transformation process

Strain	Growth Medium	Transformants	Genotype
tSWJ 2893	SM Meth Ribo	1, 2, 3, 4, 5, 6*	pyroA4 ΔnkuA::argB; methB3; riboB2
tLC 5602	SM BiPaba	7, 8, 9, 10, 10*, 11, 12*	pabaA1 yA2; snxA2::GA5::myc9::riboB; pyroA4 ΔnkuA::argB; riboB2
tAMO 5405	SM UU	13, 14, 15, 16, 17, 18*	pyrG89 yA2; pyroA4 ΔnkuA::argB; drkA1 snoA31::GA5::myc9::riboB; riboB2
tATA 5402	SM BiPaba	19, 20, 21, 22, 23, 23*, 24	pabaA1 biA1; pyroA4 ΔnkuA::argB; snoA31::GA5::myc9::riboB; riboB2

To ensure clonal purity, single colonies were streaked three times on synthetic minimal media (SM) lacking pyridoxine (Pyro) but enriched with other nutrients based on the strain.

Isolation of *Aspergillus nidulans* transformant gDNA

In order to prepare the transformant gDNA for molecular diagnosis, spores were harvested from both the transformants and the controls and grown overnight in liquid cultures at 28-32°C. Mycelia were harvested through Miracloth, washed with cold dH_2O, thoroughly pressed dry, and flash frozen before being lyophilized overnight. For each transformant, about 200 µL of powdered mycelia was suspended in 750 µL of sterile extraction buffer (50 mM Na_2EDTA, 0.25% SDS, 2 µL/mL DEPC, sterile dH_2O). The tubes were centrifuged (max. speed, 6 min, RT), the supernatants were recovered, and 0.5 volumes of 5M KOAc were added to each sample. The supernatants were mixed gently and then incubated on ice for 10 minutes. The samples were centrifuged to pellet out the proteinaceous debris (max. speed, 5 min, RT), and the supernatants were recovered and treated with 600 µL of H_2O-saturated chloroform. The tubes were shaken vigorously before being centrifuged (max. speed, 6 min, RT). The aqueous layers were removed, and each was treated with an equal volume of isopropanol (-20°C) to precipitate the DNA. Tubes were shaken, and samples were incubated on ice for 10 minutes before being centrifuged (max. speed, 20 sec, RT). Pellets were washed twice with 70% EtOH (1 mL, -20°C), residual EtOH was removed, and each pellet of transformant gDNA was dissolved in 75 µL of TE-RNAse A with heat (55°C) and gentle flicking.

Molecular diagnostics

To determine if gene replacement was successful, trans-locus PCR was performed on isolated transformant gDNA (1:10 dilution) using the Bre1 – 5' For and Bre1 – 3' Rev primers. The PCR products were electrophoresed and imaged.

To confirm the location of construct integration and ascertain whether ectopic integration occurred, a restriction digest of 10 µL of transformant gDNA was performed (*EcoRI*, 37°C, 4.5 hours). Digestion was confirmed via gel electrophoresis, and the electrophoretically separated DNA was electroblotted to a nylon membrane for Southern blot analysis, which was executed according to the manufacturer's instructions (GENIE Blotter, Idea Scientific, Minneapolis, MN). The membrane was probed with DIG-labeled *A. fumigatus pyroA* DNA, and chemiluminescent detection was performed as described in the manufacturer's protocol (DIG-High Prime DNA Labeling and Detection Kit, Roche Biomedical Products).

Phenotypic analysis

To qualitatively evaluate the effect of temperature and DNA damage agents on the growth of ΔBre1 mutants, spores were point-inoculated on plates incubated at 22°C, 29°C, or 37°C and on plates containing 0.0175% 1,2,7,8-diepoxyoctane (DEO), 25 µM camptothecin (CPT), or 0.0125% methylmethane sulfonate (MMS), which were incubated at 33°C. PCS 439 and parent strains were used as controls. All plates contained synthetic minimal media (SM) enriched with uridine/uracil (UU), biotin (Bi), para-aminobenzoic acid (Paba), pyridoxine (Pyro), methionine (Meth), and riboflavin (Ribo).

ΔBre1 intercrosses

To determine whether loss of Bre1 results in loss of meiotic ability and/or influences genetic recombination, spores from two strains were mixed vigorously in 3 mL of rich liquid media in a sterile culture tube. The crosses were grown at 33°C for 3 days until a mat of mycelia formed on the surface. The mat was removed, cut into 6 equal pieces, and plated on media that selected for the growth of the outcrossed heterokaryons while prevented growth of the parent homokaryons. Plates were incubated upright at 33°C overnight, flipped upside down the following day, and taped to restrict gas exchange on

the third day. Crosses were inverted and grown at 33°C for 7 days at which point they were examined for cleistothecia.

Results

Preparation of *Af pyroA* selectable marker

Amplification, extraction, and purification of the *Aspergillus fumigatus pyroA* selectable marker yielded the expected 1.65 kb fragment at a concentration of 0.032 µg/µL (Figure 3a).

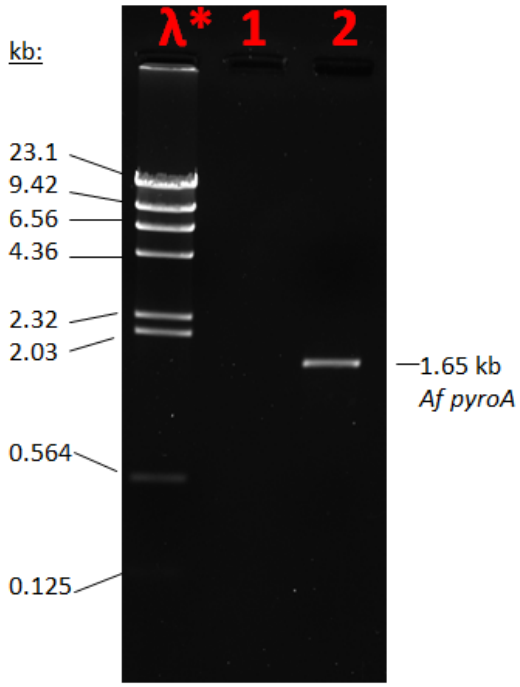

Figure 3a. Preparation of PCR-amplified *A. fumigatus* selectable marker *Af pyroA*.
PCR-amplified *Af pyroA* DNA (1.65 kb) was recovered *via* QIAEX II gel extraction. Recovered DNA (1 µL) was electrophoresed in a 1% agarose minigel to check for quality.
Key to lanes: λ*, bacteriophage lambda (λ) DNA digested with *Hind*III (0.625 µg); 1, empty; 2, recovered PCR product of *A. fumigatus pyroA* (0.032 µg).

Preparation of the Bre1 5' and 3' flanking regions

Using PCS 439 and SWJ 400 genomic DNA, the regions 5' and 3' of the *Aspergillus nidulans* Bre1 gene were amplified. The 5' and 3' regions of *Af pyroA* that were integrated into the Bre1 5' reverse primer and Bre1 3' forward primer as marker tails were also successfully amplified based on the sizes of

the resulting fragments: 1.99 kb for 5’ flank + 3’ marker tail and 2.53 kb for 3’ flank + 5’ marker tail (Figure 3b). Concentrations of 0.031 and 0.019 µg/µL were obtained for the 5’ flank and 3’ flank, respectively.

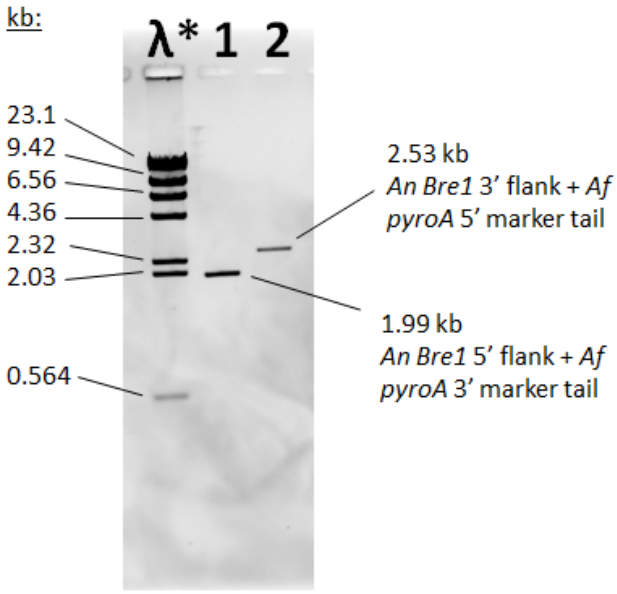

Figure 3b. Amplification and purification of *Aspergillus nidulans* Bre1 5’ flank and 3’ flanking DNA. The *A. nidulans* Bre1 5’ flank + 3’ *A. fumigatus pyroA* marker tail fragment (1.99 kb) and the *A. nidulans* Bre1 3’ flank + 5’ *A. fumigatus pyroA* marker tail fragment (2.53 kb) were amplified by PCR and electrophoresed in a 0.9% agarose gel. The 5’ flank and 3’ flank DNAs were recovered *via* QIAEX II gel extraction. 1 µL of the purified DNA was electrophoresed in a 1% agarose minigel to confirm recovery. Key to lanes: λ*, bacteriophage lambda (λ) DNA (0.625 µg) digested with *Hind*III; 1, Bre1 5’ flank + 3’ *A. fumigatus pyroA* marker tail (0.031 µg); 2, Bre1 3’ flank + 5’ *A. fumigatus pyroA* marker tail (0.019 µg).

Preparation of the three-way fusion construct for Bre1 deletion

The Bre1 5’ and 3’ flanks were combined with the *Af pyroA* selectable marker in a 1:1:3 ratio. The marker tails annealed to their complementary regions on the selectable marker, serving as primers for the DNA Phusion Polymerase, generating 2 two-way products: 5’ flank + selectable marker (3.64 kb) and 3’ flank + selectable marker (4.18 kb). The two-way products annealed via the 1.65 kb selectable marker, allowing the Phusion Polymerase to create the 6.12 kb three-way fusion construct (Figure 4).

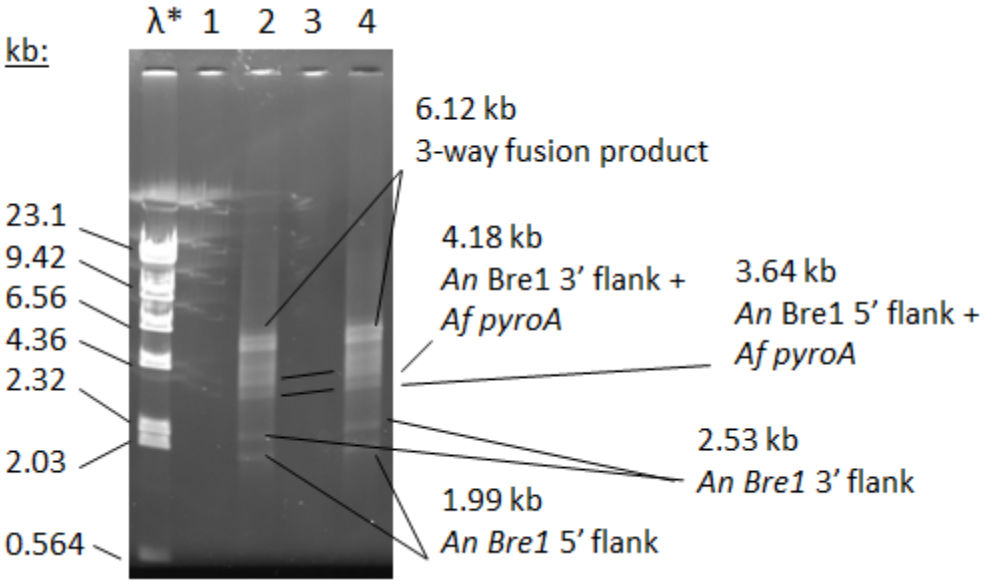

Figure 4. Generation of three-way fusion PCR product for Bre1 deletion.
Three-way fusion PCR products (6.12 kb) were amplified using the *An* Bre1 5' flank + 3' *Af pyroA* marker tail fragment (1.99 kb), the *An* Bre1 3' flank + 5' *Af pyroA* marker tail fragment (2.53 kb), and the *Af pyroA* selectable marker (1.65 kb) in a 1:1:3 ratio. 9 µL of the two PCR products were electrophoresed in a 1% agarose minigel.
Key to lanes: λ*, bacteriophage lambda (λ) DNA (0.625 µg) digested with *Hind*III; 1 and 3, empty; 2 and 4, three-way fusion PCR product, 2 two-way products (3' flank + *pyroA*, 5' flank + *pyroA*), and flanking genomic fragments.

Initial three-way fusion PCR products were amplified using nested Bre1 5' forward and 3' reverse primers. Though each of the two-way products contained a sequence complementary to one of the nested primers, only the three-way construct had sequences complementary to both nested primers; therefore, only the three-way product was amplified significantly. The 5.55 kb nested three-way fusion construct was purified for transformation into *Aspergillus nidulans* via phenol chloroform extraction (Figure 5). A concentration of 0.148 µg of the purified nested three-way construct per µL was obtained.

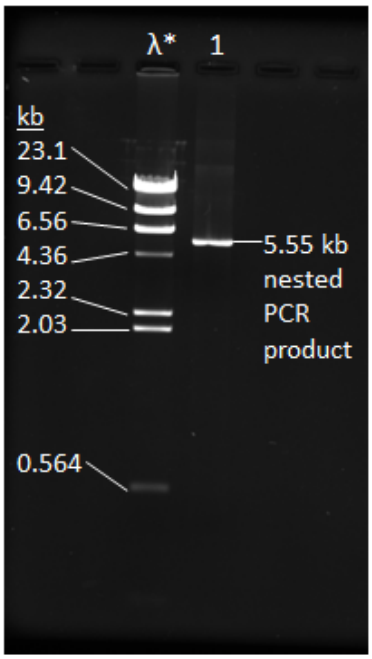

Figure 5. Amplification and purification of nested three-way fusion PCR product.
The initial three-way fusion product was amplified using nested primers. The nested three-way fusion construct (5.55 kb) was purified for transformation via phenol chloroform extraction. One µL of the purified DNA (0.148 µg) was electrophoresed in a 1% agarose minigel to check for quality.
Key to lanes: λ*, bacteriophage lambda (λ) DNA (0.625 µg) digested with *Hind*III; 1, purified nested PCR product.

Transformation of *Aspergillus nidulans* with Bre1 deletion construct

Protoplasts were made from four parent strains that are auxotrophic for pyridoxine (Table 2). After incubation with the Bre1 deletion construct, transformants were plated on media lacking pyridoxine. Only protoplasts that integrated the deletion construct into their DNA, thus providing a function copy of pyroA and allowing for the production of pyridoxine, survived on the media. Transformants were grown for seven days (Figure 6).

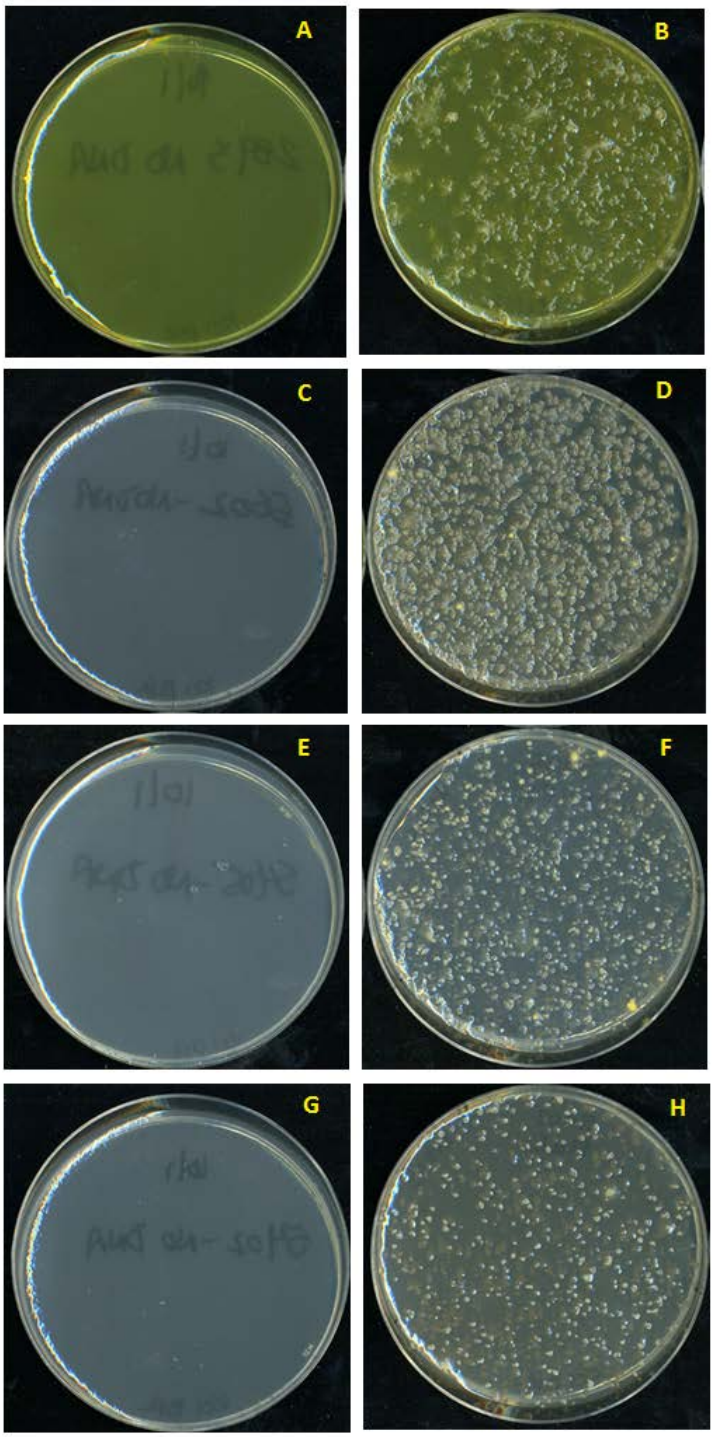

Figure 6. *Aspergillus nidulans* transformants from four parent strains.
Protoplasts from four parent strains were treated with the Bre1 deletion construct, plated, and grown for 7 days.
A-B. Strain tSWJ 2893. No DNA control (**A**), and Bre1 deletion construct transformants (**B**).
C-D. Strain tLC 5602. No DNA control (**C**), and Bre1 deletion construct transformants (**D**).
E-F. Strain tAMO 5405. No DNA control (**E**), and Bre1 deletion construct transformants (**F**).
G-H. Strain tATA 5402. No DNA control (**G**), and Bre1 deletion construct transformants (**H**).

Identification of ΔBre1 transformants

Two PCR-based techniques were used to verify genuine deletion strains. The first strategy, trans-locus PCR, used the original Bre1 5' forward and 3' reverse primers to amplify the locus in genomic DNA isolated from the *A. nidulans* transformants. Transformants that did not integrate the deletion construct at the Bre1 locus and still retain the Bre1 gene produce a 6.9 kb band, whereas those that replaced the Bre1 gene with the smaller pyroA selectable marker generate a 6.1 kb band (Figure 7a).

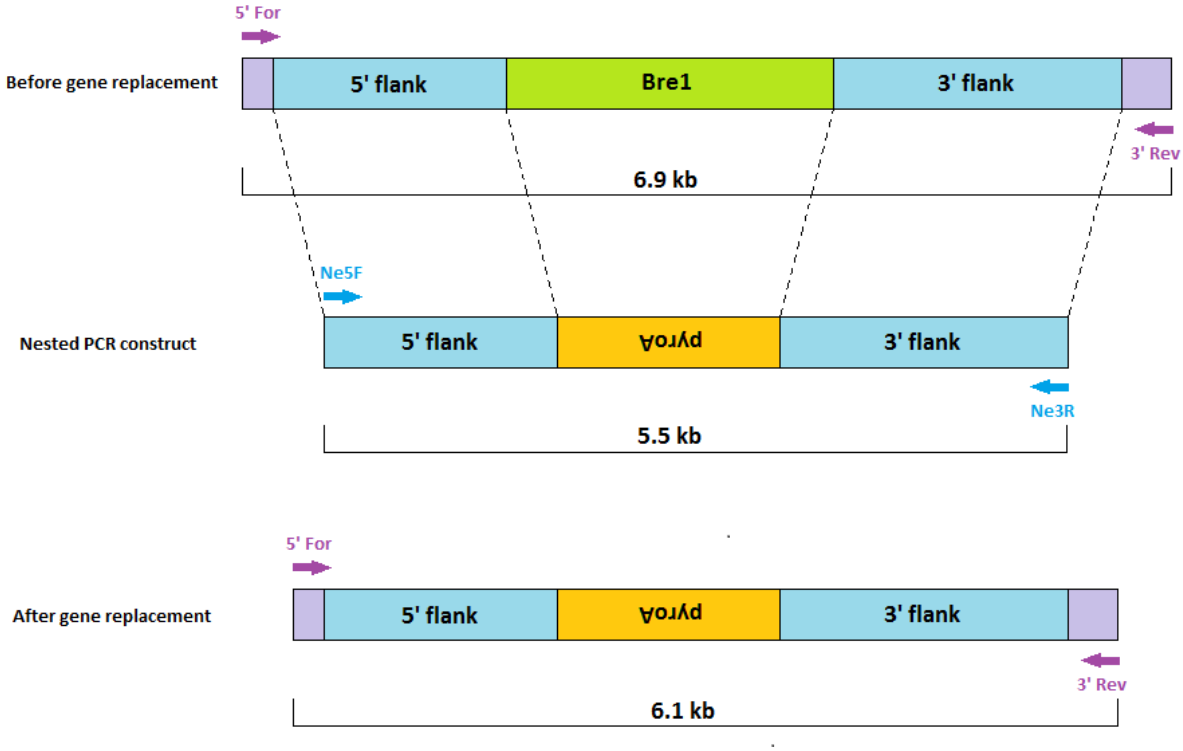

Figure 7a. Schematic diagram of the Bre1 gene replacement strategy.
Successful deletions result in a 6.1 kb band, whereas the wild type gDNA should produce a band of 6.9 kb.

The initial trans-locus PCR, in which the genomic DNA was undiluted, only yielded two transformants with bands. The gDNA was diluted by a factor of ten for the second trans-locus PCR, which succeeded in generating bands for the other transformants (Figure 7b). Samples 2893-1, 5405-13,

5405-14, 5405-15, 5402-22, and 5402-23 exhibit the diagnostic PCR pattern: a smaller (6.1 kb) translocus product. The wild type controls and samples 2893-3, 2893-4, 5602-9, 5602-11, 5402-21 all exhibit PCR patterns with a larger (6.9kb) translocus product, indicating that the Bre1 gene is still intact. Samples 2893-2, 5602-7, 5602-12*, and 5402-19 exhibit both bands, indicative of a diploid organism in which one nucleus carries the deletion and the other does not. Samples 5602-8 and 5405-18* exhibit neither of the PCR patterns expected but, like several other samples and one of the controls, show a product of about 3 kb that suggests that the translocus primers may be binding nonspecifically (Figure 7b).

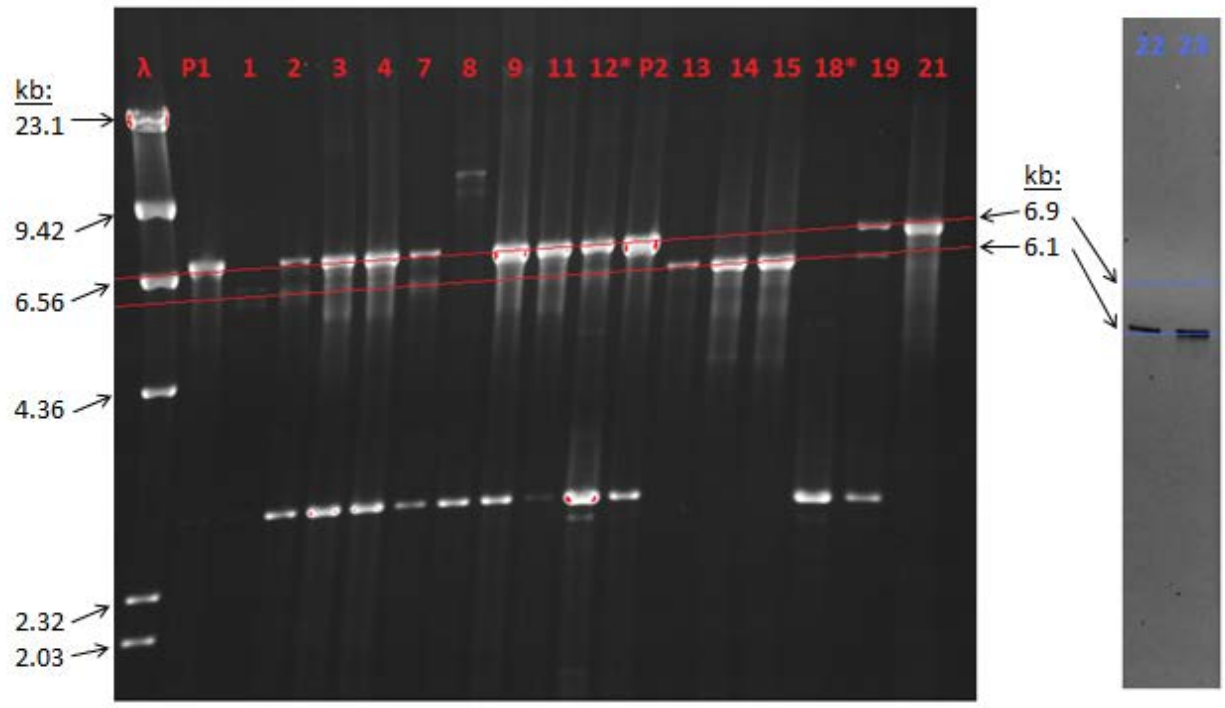

Figure 7b. ΔBre1 trans-locus PCR.

gDNA from *A. nidulans* ΔBre1 transformants was amplified using 5' For and 3' Rev primers. The PCR products (15 µL) were electrophoresed in 0.9% agarose gels and stained with EtBr. Left: ΔBre1 gDNA 10x dilution; Right: ΔBre1 gDNA undiluted.

Key to lanes: λ, bacteriophage lambda (λ) DNA (0.625 µg) digested with *Hind*III; P1, wild type control gDNA PCS 439; 1-4, 2893-1, 2893-2, 2893-3, 2893-4, respectively; 7-12*, 5602-7, 5602-8, 5602-9, 5602-11, 5602-12*, respectively; P2, wild type control gDNA PCS 439; 13-18*, 5405-13, 5405-14, 5405-15, 5405-18*, respectively; 19-23, 5402-19, 5402-21, 5402-22, 5402-23, respectively.

The second strategy used to identify ΔBre1 transformants, restriction digestion followed by Southern blotting, took advantage of the location of an *EcoRI* restriction site within the *pyroA* gene relative to the two flanking *EcoRI* restriction sites that fell outside the endpoints of the deletion construct. When treated with a labeled *pyroA* probe, a genuine deletion strain produces a 4.6 kb band with a 3.4 kb band; a different pattern of bands is indicative of ectopic integration (Figure 8a).

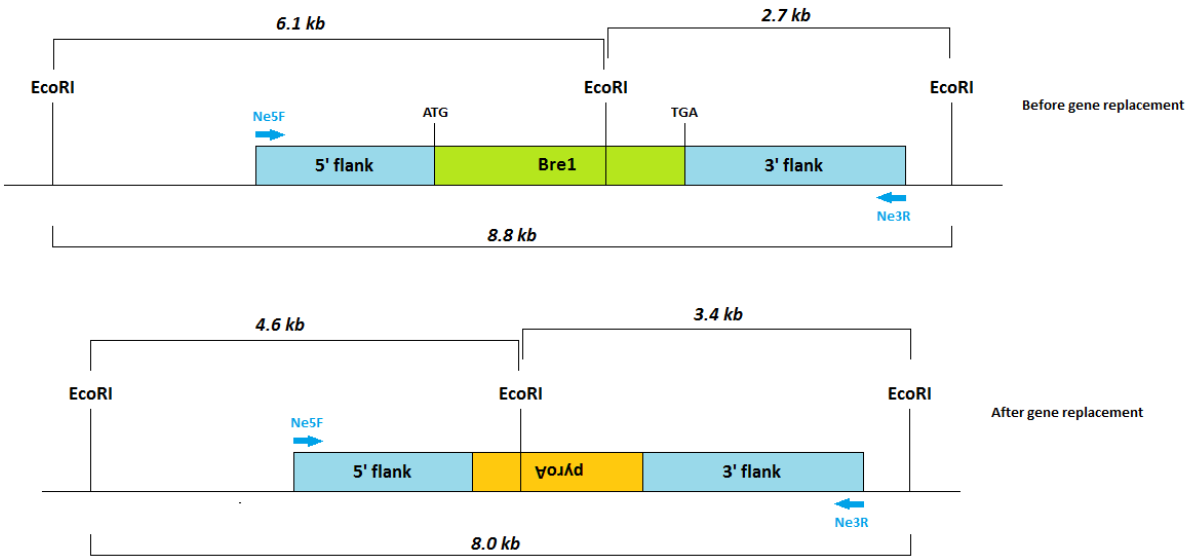

Figure 8a. Strategy for Southern blotting of ΔBre1 transformants.
EcoRI digest probed with *Af pyroA* should produce two diagnostic bands of 4.6 and 3.4 kb in Bre1 deletions.

The restriction digests were electrophoresed, and ethidium bromide staining indicated that *EcoRI* successfully fragmented the gDNA of the transformants (Figure 8b).

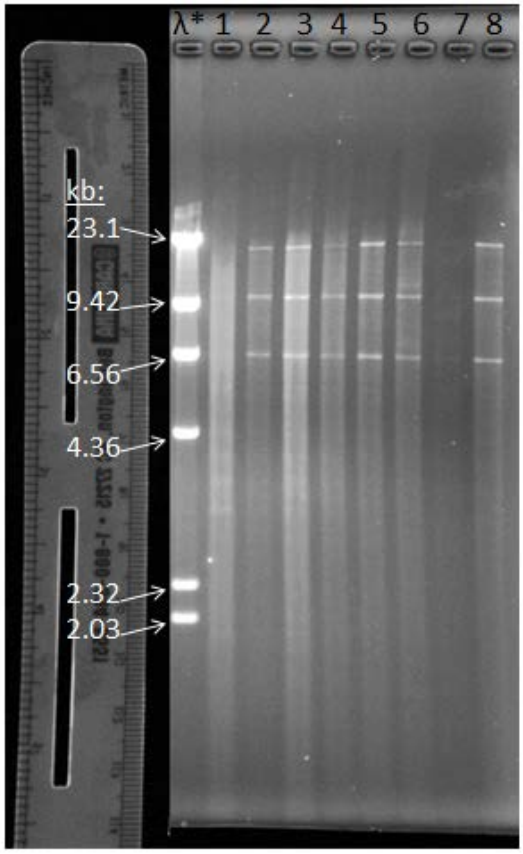

Figure 8b. *EcoR*I digestion of *Aspergillus nidulans* ΔBre1 gDNA.
gDNA from *A. nidulans* ΔBre1 transformants was extracted, purified, and then 10 µL of each was digested with *EcoR*I at 37 °C for 5 hours. The digestion reactions (33 µL) were electrophoresed in a 0.9 % agarose gel and stained with EtBr.
Key to lanes: λ*, bacteriophage lambda (λ) DNA (1.25 µg) digested with *Hind*III; 1, wild type control gDNA PCS 439; 2, 2893-1; 3-6, 5405-13, 5405-14, 5405-15, 5405-16, respectively; 7-8, 5402-22 and 5402-23, respectively.

The digested, electrophoresed gDNA was electroblotted onto a nylon membrane and probed with DIG-labeled *Af pyroA*, which can be detected *chemiluminescently.* The transformants did not exhibit any detectable Southern blot pattern. The lack of bands on the Southern blot suggests a technical flaw in the Southern blot reagent or procedure (Figure 8c).

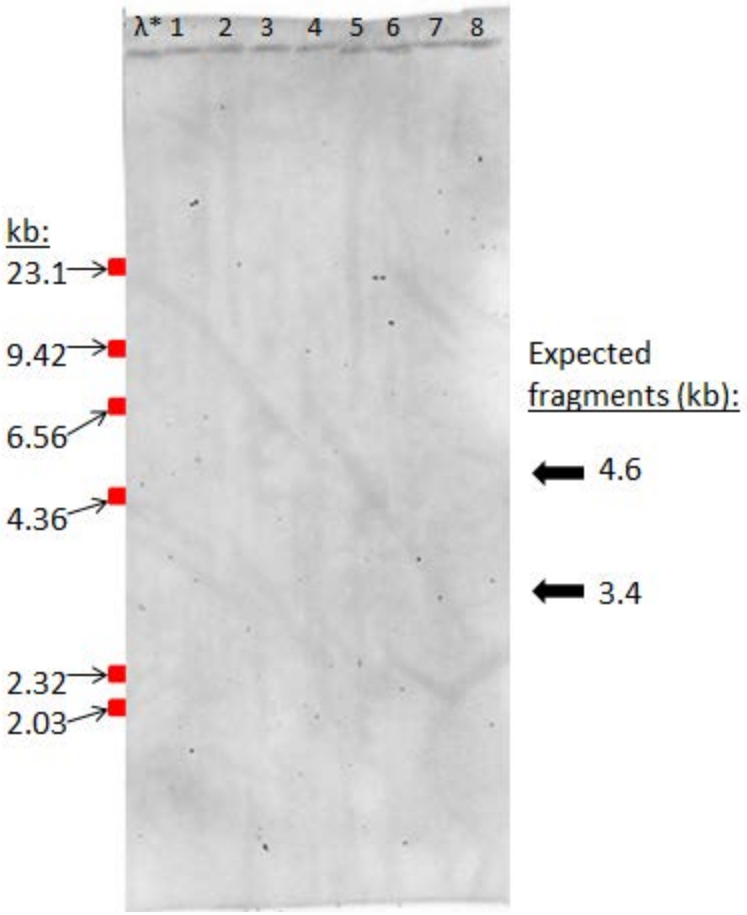

Figure 8c. ΔBre1 Southern blot.

EcoRI digested gDNAs were transferred to a nylon membrane and probed with DIG-labeled *A. fumigatus pyroA* DNA. Chemiluminescent detection was performed according to manufacturer's recommendation (DIG-high prime DNA labeling and detection kit, Roche Biomedical Products)

Key to lanes: λ*, bacteriophage lambda (λ) DNA digested with *Hind*III; 1, wild type control gDNA PCS 439; 2, 2893-1; 3-6, 5405-13, 5405-14, 5405-15, 5405-16, respectively; 7-8, 5402-22 and 5402-23, respectively.

The lack of bands on the Southern blot is inconclusive and cannot be used to diagnose successful deletion. However, the trans-locus PCR indicates genuine ΔBre1 strains were obtained (Table 3).

Table 3. Strain table for verified ΔBre1 transformants

Strain	ΔBre1 Transformant	Genotype
tMAA 5656	tSWJ 2893 - 1	ΔBre1::pyroA; pyroA4 ΔnkuA::argB; methB3; riboB2
tMAA 5657	tAMO 5405 - 13	pyrG89 ΔBre1::pyroA yA2; pyroA4 ΔnkuA::argB; drkA1 snoA31::GA5::myc9::riboB; riboB2
tMAA 5658	tAMO 5405 - 14	pyrG89 ΔBre1::pyroA yA2; pyroA4 ΔnkuA::argB; drkA1 snoA31::GA5::myc9::riboB; riboB2
tMAA 5659	tAMO 5405 - 15	pyrG89 ΔBre1::pyroA yA2; pyroA4 ΔnkuA::argB; drkA1 snoA31::GA5::myc9::riboB; riboB2
tMAA 5660	tATA 5402 - 22	pabaA1 ΔBre1::pyroA biA1; pyroA4 ΔnkuA::argB; snoA31::GA5::myc9::riboB; riboB2
tMAA 5661	tATA 5402 - 23	pabaA1 ΔBre1::pyroA biA1; pyroA4 ΔnkuA::argB; snoA31::GA5::myc9::riboB; riboB2

Effect of temperature and DNA damage agents on ΔBre1 transformants

Temperature sensitivity was assessed through point-inoculation of ΔBre1 spores onto plates and stored at various temperatures; DNA damage response was examined via point-inoculation of ΔBre1 spores onto plates containing DNA damage agents and stored at 33°C (Figure 9). Although ΔBre1 mutants are usually slow growing and sickly, in all cases these deletants appear to have an increased sensitivity to lower temperatures and DNA damage agents (Figure 9).

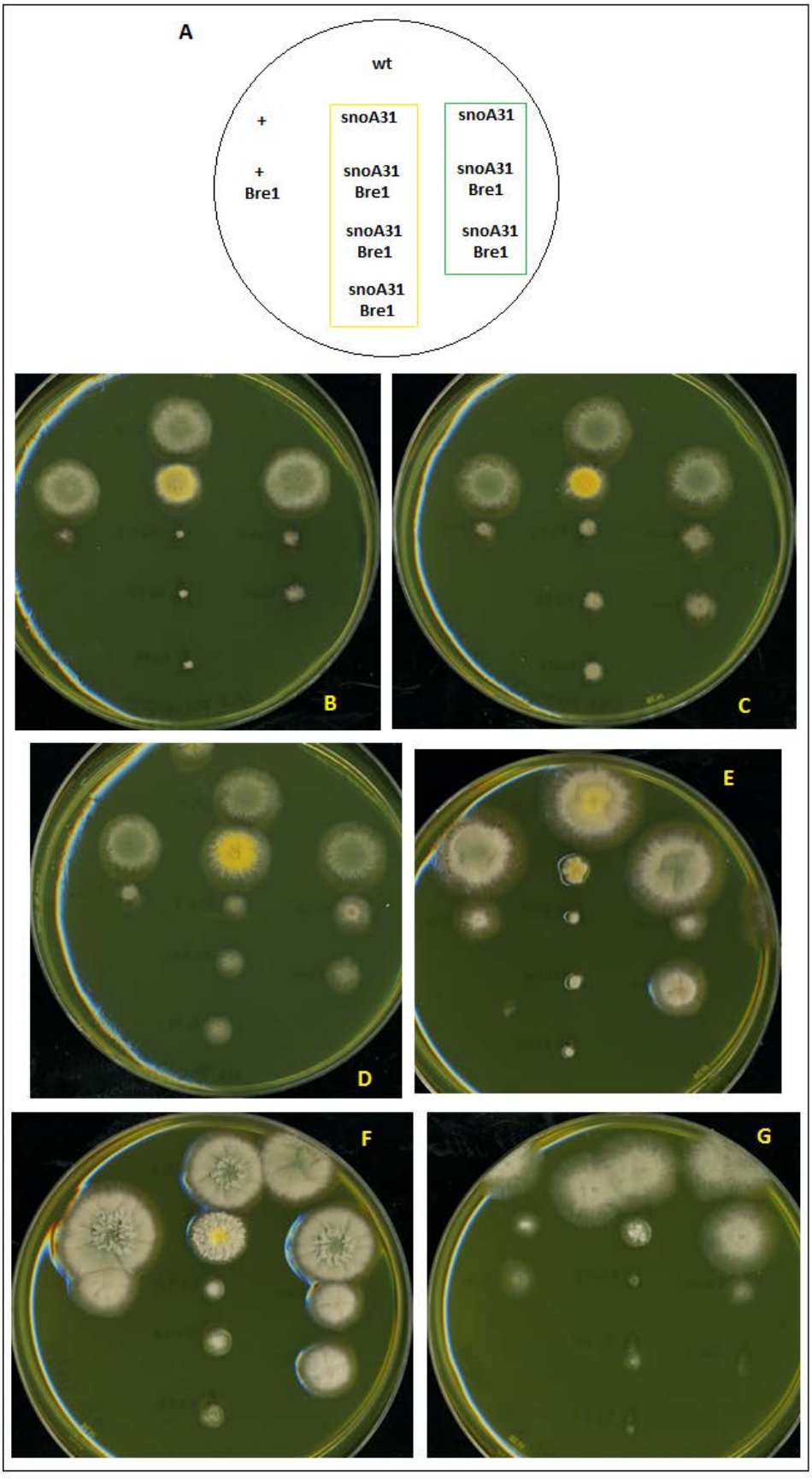
A
wt
+
+
Bre1
snoA31
snoA31
Bre1
snoA31
Bre1
snoA31
Bre1
snoA31
snoA31
Bre1
snoA31
Bre1
B
C
D
E
F
G

Figure 9. DNA damage agent assay of ΔBre1 transformants.

A. Key to plates: (*TOP*) wt = PCS 439; (*LEFT COLUMN*) + = tSWJ 2893; +/Bre1 = tMAA 5656; (*MIDDLE COLUMN*) snoA31 = tAMO 5405; snoA31/Bre1 = tMAA 5657 (top), tMAA 5658 (middle), tMAA 5659 (bottom); (*RIGHT COLUMN*) snoA31 = tATA 5402; snoA31/Bre1 = tMAA 5660 (top), tMAA 5661 (bottom). **B-D.** Temperature sensitivity assay. Synthetic minimal media enriched with uridine, uracil, biotin, methionine, para-aminobenzoic acid, pyridoxine, and riboflavin incubated at 22°C (**B**), 29°C (**C**), or 37°C (**D**).

E-G. DNA damage agent assay. Synthetic minimal media enriched with uridine, uracil, biotin, methionine, para-aminobenzoic acid, pyridoxine, and riboflavin. Plates contained 0.0175% DEO (**E**), 25 μM CPT (**F**), or 0.0125% MMS (**G**), and were incubated at 33°C.

Genetic analysis of meiotic recombination

Genetic crosses were performed between ΔBre1 transformants in an attempt to determine whether loss of Bre1 results in loss of meiotic ability and whether ΔBre1 mutants exhibit suppressive or additive genetic interactions with snoA31 mutants. However, no cleistothecia were formed from crosses between two ΔBre1 strains. Only the cross between a ΔBre1 strain and a control snxA2 strain produced a few cleistothecia (Table 4).

Table 4. Crosses between ΔBre1 transformants

Cross	Parent Strains	Key Genotypic Features	Selective Growth Medium	Cleistothecia Formation
1	tMAA 5656 X tLC 5602	ΔBre1 (methB3; riboB2) X snxA2 (pabaA1; pyroA4)	SM Meth Paba	Some
2	tMAA 5660 X tMAA 5657	ΔBre1 snoA31 (pabaA1 biA1) X ΔBre1 snoA31 (pyrG89)	SM Paba	No
3	tMAA 5661 X tMAA 5658	ΔBre1 snoA31 (pabaA1 biA1) X ΔBre1 snoA31 (pyrG89)	SM Paba	No
4	tMAA 5659 X tMAA 5656	ΔBre1 snoA31 (pyrG89) X ΔBre1 (methB3; riboB2)	SM Ribo	No

Discussion

In this experiment, a three-way fusion construct was used to delete the Bre1 gene from *Aspergillus nidulans*, as confirmed by trans-locus PCR, and effects of the deletion on mitotic growth, temperature sensitivity, DNA damage response, and meiotic viability were examined. A qualitative comparison between deletion and parental strains indicate that ΔBre1 mutants have a decreased rate of

mitotic growth, as determined by the smaller colonies and slowed rate of formation of reproductive spores. The DNA damage assay indicates that ΔBre1 strains are more sensitive to colder temperatures as well as DNA damage agents. Intercrossing suggested that the Bre1 deletants are unable to undergo meiosis.

The molecular diagnosis of Bre1 deletion was based entirely on the trans-locus PCR due to technical flaws in the Southern blot reagent or procedure. While the absence of bands on the Southern blot would suggest that none of the strains integrated the *pyroA* selectable marker, the unambiguous diagnostic PCR pattern exhibited by certain transformants, coupled with the qualitative differences in colony size/reproductive spore formation, indicates that the Southern blot is flawed, and its data should be disregarded. Though the trans-locus PCR suggests that genuine deletion strains were obtained, prevalence of ectopic integration cannot be conclusively determined without Southern blot analysis. A Southern blot that probed for the Bre1 gene directly could be used to definitively prove the gene was deleted; the lack of a band in ΔBre1 transformants would support the deletion identity of the strains. However, it is possible that slowed, impaired growth of the ΔBre1 mutants resulted in gDNA that is unsuitable for standard Southern blot procedures.

The severe developmental impact of ΔBre1 *A. nidulans* transformants stems from its role as a regulator for multiple cellular processes. Ubiquitination at histone H2B-K123 promotes methylation of K4 and K79 of histone H3, and these post-translational modifications are necessary for active transcription, DNA damage repair pathways, optimal mitotic growth, and meiosis [1-3]. Previous studies have established that Rad6 and H2B-K123R mutants show pronounced mitotic and meiotic defects [12]. Mitotic growth was characterized by reduced colony size on plates, which approximated to a 30% increase in doubling time in liquid medium [12]. This is consistent with the function of Bre1 as a key component of the complex that recruits RNA polymerase to actively transcribed regions; loss of Bre1 impairs processive transcription. Additionally, the Rad6-Bre1 pathway functions upstream of Cdc28, the

cyclin-dependent kinase that is both necessary and sufficient for cell cycle regulation in *S. cerevisiae*, by promoting expression of early cyclins [13]. Loss of Bre1 impairs the expression of the early cyclins, resulting in cell cycle delays. These results indicate that the Rad6-Bre1-dependent ubiquitination of H2B-K123 is required for optimal mitotic development.

The absence of sexual fruiting bodies (cleistothecia) in ΔBre1 intercrosses suggests that Bre1 is necessary for meiosis in *A. nidulans*. This result is consistent with other findings that intercrosses between Rad6/H2B-K123R mutants resulted in homozygous mutant diploids that were unable to form ascospores [12, 22]. While Rad6 does influence many different cellular processes, the H2B-K123R mutant is phenotypically equivalent to the Rad6 mutant in regard to meiosis and cleistothecium formation; H2B-K123R mutants were blocked at the S or G2/M phase prior to the first meiotic division and, as such, were unable to form ascospores [12]. Additionally, ΔBre1 and H2B-K123R mutants showed reduced formation of double strand breaks (DSB) in meiosis, which indicates that histone H2B-K123 ubiquitination is potentially involved in meiotic DSB formation through promoting recruitment and/or stabilization of DSB forming machinery [23]. These results support that the role of Bre1 as a regulator of meiosis is exercised via ubiquitination of histone H2B-K123.

The susceptibility of ΔBre1 *A. nidulans* mutants to DNA damage agents is not unprecedented; the Bre1 gene was discovered when *Saccharomyces cerevisiae* deletion strains were screened for reduced growth when exposed to brefeldin A [14]. Previous studies have established that histone H3-K79 methylation is necessary for initiating the DNA repair response, and since histone H2B-K123 ubiquitination is required for methylation of histone H3-K79, loss of Bre1 impairs the DNA damage response [3, 24]. Though there did appear to be some increased sensitivity to lower temperatures, it may just be the result of subjecting already slow-growing strains to less-than-optimal growing temperatures.

Though the double mutant is meiotically defective, an in-depth exploration into the haplosufficiency of the single mutant heterokayron to initiate meiotic recombination would help

elucidate the extent to which Bre1 influences meiotic DSB formation. Furthermore, investigation into whether exogenous *A. nidulans* Bre1 protein could resolve the meiotic block in the double mutants would verify that the loss of Bre1 is the source of the block, and potentially illuminate other epigenetic regulators active in germ cells.

Literature Cited

[1] Wood A, Krogan NJ, Dover J, Schneider J, Heidt J, Boateng MA, Dean K, Golshani A, Zhang Y, Greenblatt JF, et al. 2003. Bre1, an E3 ubiquitin ligase required for recruitment and substrate selection of Rad6 at a promoter. Molecular Cell 11:267–274.

[2] Kim J, Roeder RG. 2009. Direct Bre1-Paf1 complex interactions and RING finger-independent Bre1-Rad6 interactions mediate histone H2B ubiquitylation in yeast. Journal of Biological Chemistry 284:20582–20592.

[3] Game JC, Williamson MS, Spicakova T, Brown JM. 2006. The RAD6/BRE1 histone modification pathway in Saccharomyces confers radiation resistance through a RAD51-dependent process that is independent of RAD18. Genetics 173:1951–1968.

[4] Song Y-H, Ahn SH. 2010. A bre1-associated protein, large 1 (Lge1), promotes h2b ubiquitylation during the early stages of transcription elongation. Journal of Biological Chemistry 285:2361–2367.

[5] Wood A, Schneider J, Dover J, Johnston M, Shilatifard A. 2003. The Paf1 complex is essential for histone monoubiquitination by the Rad6-Bre1 complex, which signals for histone methylation by COMPASS and Dot1p. Journal of Biological Chemistry 278:34739–34742.

[6] Hahn MA, Dickson K-A, Jackson S, Clarkson A, Gill AJ, Marsh DJ. 2012. The tumor suppressor CDC73 interacts with the ring finger proteins RNF20 and RNF40 and is required for the maintenance of histone 2B monoubiquitination. Human Molecular Genetics 21:559–568.

[7] Lee J-S, Shukla A, Schneider J, Swanson SK, Washburn MP, Florens L, Bhaumik SR, Shilatifard A. 2007. Histone Crosstalk between H2B Monoubiquitination and H3 Methylation Mediated by COMPASS. Cell 131:1084–1096.

[8] Latham JA, Chosed RJ, Wang S, Dent SYR. 2011. Chromatin signaling to kinetochores: Transregulation of Dam1 methylation by histone H2B ubiquitination. Cell 146:709–719.

[9] Vitaliano-Prunier A, Menant A, Hobeika M, Géli V, Gwizdek C, Dargemont C. 2008. Ubiquitylation of the COMPASS component Swd2 links H2B ubiquitylation to H3K4 trimethylation. Nature Cell Biology 10:1365–1371.

[10] Fingerman IM, Li H-C, Briggs SD. 2007. A charge-based interaction between histone H4 and Dot1 is required for H3K79 methylation and telomere silencing: Identification of a new trans-histone pathway. Genes and Development 21:2018–2029.

[11] Game JC, Chernikova SB. 2009. The role of RAD6 in recombinational repair, checkpoints and meiosis via histone modification. DNA Repair 8:470–482.

[12] Robzyk K, Recht J, Osley MA. 2000. Rad6-dependent ubiquitination of histone H2B in yeast. Science 287:501–504.

[13] Zimmermann C, Chymkowitch P, Eldholm V, Putnam CD, Lindvall JM, Omerzu M, Bjørås M, Kolodner RD, Enserink JM. 2011. A chemical-genetic screen to unravel the genetic network of CDC28/CDK1 links ubiquitin and Rad6-Bre1 to cell cycle progression.

[14] Murén E, Oyen M, Barmark G, Ronne H. 2001. Identification of yeast deletion strains that are hypersensitive to brefeldin A or monensin, two drugs that affect intracellular transport. Yeast 18:163–172.

[15] Rieger K-J, El-Alama M, Stein G, Bradshaw C, Slonimski PP, Maundrell K. 1999. Chemotyping of yeast mutants using robotics. Yeast 15:973–986.

[16] Kim J, Hake SB, Roeder RG. 2005. The human homolog of yeast BRE1 functions as a transcriptional coactivator through direct activator interactions. Molecular Cell 20:759–770.

[17] BRE1 (YDL074C) Interaction Summary | BioGRID. Available from: http://thebiogrid.org/31987/summary/saccharomyces-cerevisiae/bre1.html

[18] brl2 (SPCC970.10c) Interaction Summary | BioGRID. Available from: http://thebiogrid.org/275874/summary/schizosaccharomyces-pombe/brl2.html

[19] RNF20 Interaction Summary | BioGRID. Available from: http://thebiogrid.org/121119/table/homo-sapiens/rnf20.html

[20] Rnf20 (RP23-134A17.1) Interaction Summary | BioGRID. Available from: http://thebiogrid.org/224649/summary/mus-musculus/rnf20.html

[21] NCU07544 Interaction Summary | BioGRID. Available from: http://thebiogrid.org/1976859/summary/neurospora-crassa/ncu07544.html

[22] Cox BS, Parry JM. 1968. The isolation, genetics and survival characteristics of ultraviolet light-sensitive mutants in yeast. Mutation Research - Fundamental and Molecular Mechanisms of Mutagenesis 6:37–55.

[23] Yamashita K, Shinohara M, Shinohara A. 2004. Rad6-Bre1-mediated histone H2B ubiquitylation modulates the formation of double-strand breaks during meiosis. Proceedings of the National Academy of Sciences of the United States of America 101:11380–11385.

[24] Cui L, Li W. 2010. Role of ubiquitination in meiotic recombination repair. Science China Life Sciences 53:447–454.